Nuclear Science and Techniques **22** (2011) 245–250

Influencing factors on local reduction of graphene oxide with a heated AFM tip

WU Zhongliang[1,2] SHEN Yue[2] ZHOU Xingfei[1,*] GUO Shouwu[3] ZHANG Yi[2,*]

[1]*Ningbo University*, *Zhejiang 315211*, *China*

[2]*Shanghai Institute of Applied Physics*, *Chinese Academy of Sciences*, *Shanghai 201800*, *China*

[3]*Research Institute of Micro/Nano Science and Technology*, *Shanghai Jiao Tong University*, *Shanghai 200240*, *China*

Abstract In this paper, the factors influencing the local thermal reduction of graphene oxide (GO) sheets are investigated. The lateral force microscopy and scanning polarization force microscopy verify that the heated tips of atomic force microscope (AFM) can thermally reduce the GO into electrical conductive nanostructures. The tip temperature, heating time, and loading force applied by the AFM tip are found to have important effects on the thermal reduction of GO, while the environmental humidity is negligible.

Key words Graphene oxide, Atomic force microscope, Heatable tip, Reduction

1 Introduction

Graphene, a 2D sheet of sp^2-hybridized carbon, has interest many researchers[1–11]. Great efforts have been made in studying its distinctive electronic, optical, magnetic, thermal, and mechanical properties, aimed at potential applications of graphene in various kind of devices[8,9,12], such as micro-electronics, sensors [13– 18], functional composites[11,19], transparent electrodes for displays[9,20–22], and solar batteries[23–25].

Graphene oxide (GO) as an important precursor for large-scale synthesis of free-standing graphene sheets[21,26,27] is electrically insulating. To make it electrically active[11,28], the GO is conducted mostly by using chemical reduction or thermal treatment[26, 29, 30]. A common way to reduce a GO sheet is to expose it to hydrazine[11,21,31–33]. After thermal annealing at 200 to 500ºC, the electrical properties can be improved[20,34].

To exploit the broad application of graphene, a key issue is to pattern the graphene-related materials in nanometer scale. Many methods[21,22,35–38], including scanning-probe-based nanolithography techniques [39], have been used. Recently, Wei *et al.*[39] reported that a heated tip of atomic force microscope (AFM) can locally reduce the GO, and pattern nanoscale areas of the reduced GO sheet at high speed. The technique, which was well related to thermal nanolithography with heated AFM tips, can locally induce chemical reactions[40–43], deposit material on a surface[44–46], and modify a polymer film[47]. However, the factors influencing the local thermal reduction of GO sheets have not been fully explored. In this paper, factors affecting local thermal reduction of GO sheets are studied with a heated AFM tip. It was found that the tip temperature, heating time, and loading force applied by the AFM tip affected the thermal reduction of GO greatly.

2 Materials and Methods

The GO sheets were synthesized by oxidizing graphite powder using $KMnO_4/H_2SO_4$, followed by ultra- sonication in water[29,48–50]. The as-synthesized GO mixture was repeatedly washed using pure water and separated through filtration. The mixture was dispersed in water (0.5 mg/mL) to prepare GO sheets by drop-cast on a mica substrate. Dried by nitrogen gas, the GO sheets were ready for uses.

The GO sheets were locally reduced and characterized with a multimode AFM (Nanoscope IIIa,

---

* Corresponding author. *E-mail address*: zhangyi@sinap.ac.cn; zhouxingfei@nbu.edu.cn

Received date: 2011-05-04

Veeco, Santa Barbara, USA) equipped with a J scanner using heatable silicon AFM probes (VITA-MM-NANOTA-200, Veeco, Santa Barbara, USA). The tip temperature was controlled with a power supply (DH1719A-5, Da Hua, Beijing, China), and was calibrated using Veeco-provided standard polymers of polycaprolactone (PCL), polyethylene (PE), and poly(ethylene terephthalate) (PET) with melting points of 55, 116, and 235°C[54], respectively. To reduce the GO locally, the AFM tip was heated when it was scanning over the surfaces of GO sheet in contact mode at a speed of several μm/s[28,42]. The local reduction was normally done with a sufficient loading force calculated from the Hooke's law, $F=k\Delta Z$, where k is the cantilever's spring constant, and ΔZ is the cantilever deflection, which can be obtained from a force curve before local reduction.

Tapping mode AFM, lateral force microscopy (LFM)[52], and scanning polarization force microscopy (SPFM)[53,54] were employed to characterize the locally reduced GO. Silicon cantilevers (NP-STT10, Veeco) with a nominal spring constant of 0.58N·m^{-1} was used in LFM. The SPFM was performed on a Multimode V AFM (Veeco, Santa Barbara, USA) equipped with a J scanner, using conductive Pt/Ti-coated silicon cantilevers with spring constant of 3.5 N·m^{-1}(NSC18/TI-PT, MikroMash).

3 Results and Discussion

3.1 Calibration of tip temperature

The GO sheets were reduced at a given temperature, the AFM tip temperature was calibrated by analyzing force curves of the heated AFM tip when it was approaching and departing from a polymer sample, based on the fact that the tip force changes dramatically when the tip temperature is higher than melting points of a polymer standard. Fig.1(A) shows the force curves with the tip on PCL. When the tip temperature was lower than melting point of PCL, the force curve was in normal jump-to-contact and pull-off transitions, but changed gradually with the tip was heated by the power supply. At certain temperature, the polymer in contact with the tip began to melt, and the tip penetrated into the surface deeply, resulting in an extended jump-to-contact transition and a large pull-off force in the force curve (the fine dotted line in Fig.1A). In this way, heating voltage corresponding to a tip temperature of the PCL melting point can be determined. Similar procedures were conducted on PE (Fig.1B) and PET (Fig.1C). Then, the tip temperatures were plotted as a function of heating voltage (Fig.1D).

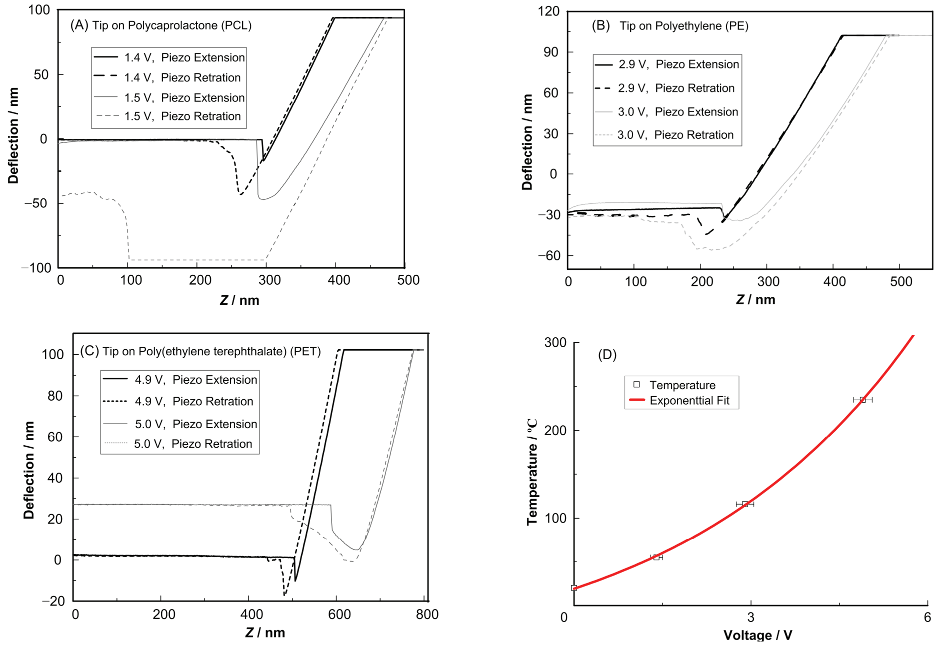

Fig.1 Force curves to calibrate the AFM tip temperature (A–C) and the standard curve (D) of the tip temperature versus heating voltage, obtained from the heating voltages at which the polymers were melted. The first spot in Fig.1(D) represents 20ºC at 0 V.

3.2 Effect of tip temperature on local reduction

Tip temperature affects greatly the local thermal reduction of GO. An AFM measurement using the local reduction showed that the GO sheet (about 1-nm thick) decreased by several angstroms. As shown in Fig.2(A), the local reduction can be realized at a tip temperature of 100°C or higher. Raster scanning by the heated AFM tip in contact mode within an area of 200 nm × 200 nm resulted in the concave square of 0.15 nm depth. The tip temperature rising could deepen the squares by 0.23–0.31 nm, indicating the GO at these areas underwent a high degree reduction [28]. Setting the tip temperature at 270°C or higher, however, the GO sheet would be torn, exposing the bare mica surface (Fig.2B). It was found that the local reduction of GO was only achieved at the hot-tip scanned area, and nearby regions to to scanned area showed no sign of damage, i.e. the heat radiation effect is negligible.

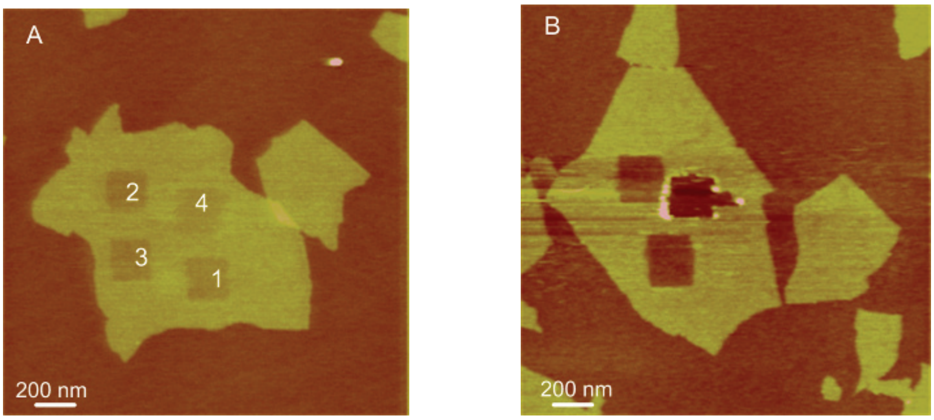

Fig.2 (A) a GO single-layer in AFM image was locally and thermally reduced by the heated AFM tip over the squares (200 nm × 200 nm). The tip temperature was 240ºC (1), 210ºC (2), 175ºC (3), and 80ºC (4), respectively, and the loading force applied by the hot AFM tip was about 100 nN. (B) The GO in AFM image was destroyed in the regions heated by a tip in high temperature of 270ºC.

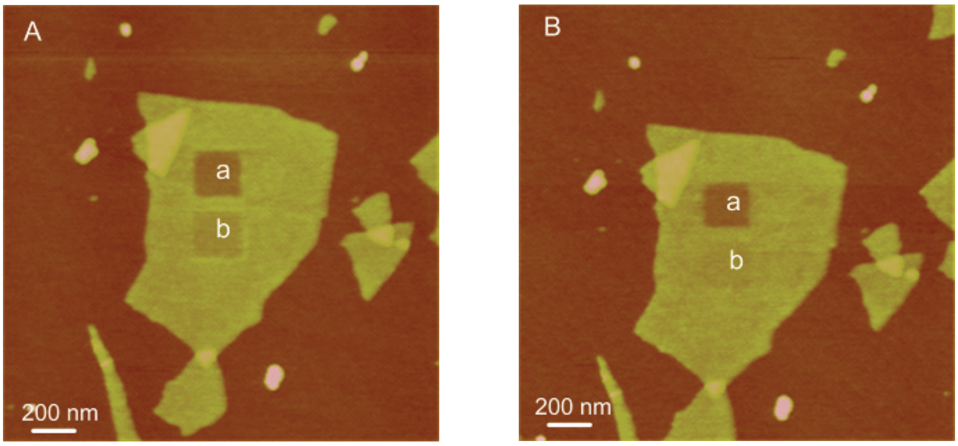

Fig.3 The effect of force on the local thermal reduction of a GO sheet in AFM images. (A) **a** region was scanned by a 210°C tip; and **b,** by an unheated tip. In both case, a force of 145 nN was applied during AFM scanning. (B) AFM image indicating that the square made by an unheated tip disappeared after 25 times scanning of an unheated tip.

3.3 Effect of force on the local reduction of GO

The tip force on the GO sheet is important for the local thermal reduction. The minimum loading force should be about 40 nN, other- wise the heated AFM tip would disengage from the sample surface, resulting in failure of the local reduction. Also, the GO sheet can be torn by too large loading force. So, a force of 80–160 nN is suitable for local reduction of GO sheets.

A cool AFM tip with sufficient loading force reduced the GO sheet locally into a less concave feature (**b** of Fig.3A) than a heated tip did (**a** of Fig.3A). Moreover, the force-generated feature disappeared after several scans of cool tip over the imaged area, but the thermally generated feature remained intact (Fig.3B). This indicates that the local thermal reduction probably leads to an irreversible chemical conversion of the GO sheet rather than mechanical removal, thus losing the oxygen-rich functional groups on the GO surface.

3.4 Effect of heating time on local reduction of GO

Scanning a GO sheet with a heated tip for longer time, the GO receives more energy, hence higher degree of its reduction. In Fig.4(A), the local regions of **a** to **d** were thermally reduced in different time periods, and the GO sheet recessed with the heating time, indicating a higher local reduction degree.

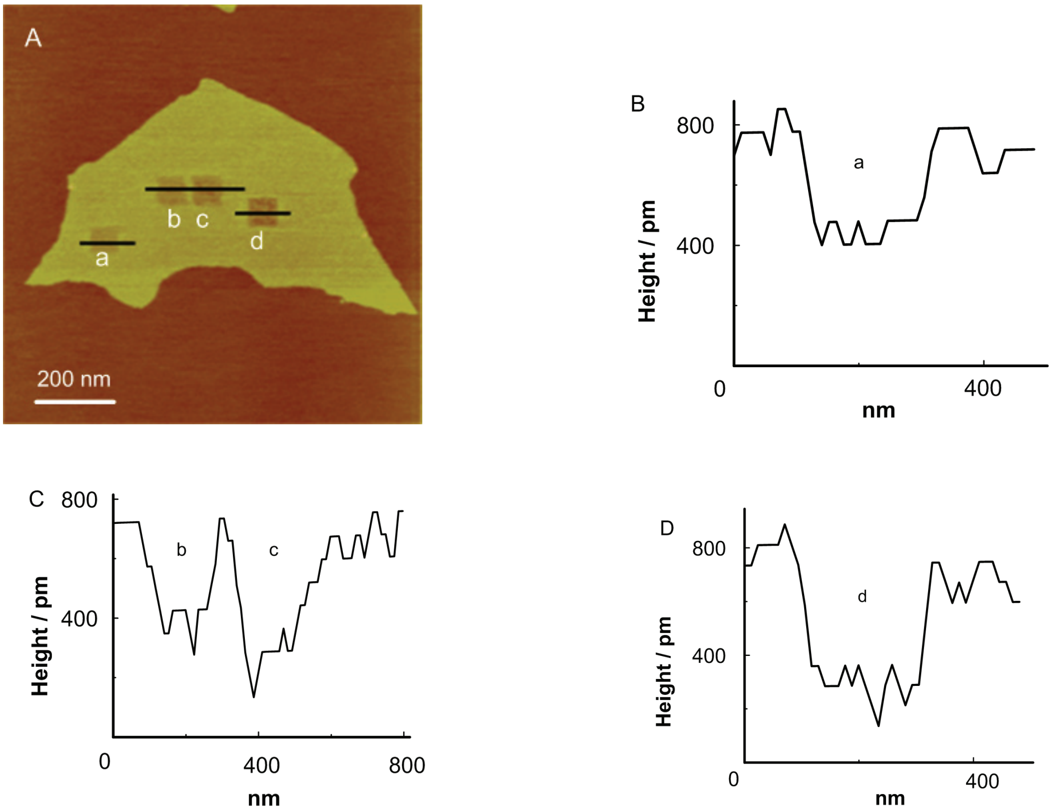

Fig.4 Effect of heating time at the constant loading force and tip temperature. (A) the four reduction regions of 200 nm × 200 nm were scanned by a 210°C tip using the scanning rate of 800 nm/s, and the scanning times is 2 for **a**; 4, for **b**; 8, for **c**; 12 for **d**. The line profiles in Fig.4(B)–4(D) correspond to the four regions of **a** to **d**, indicating that GO reduction degree increases with heating.

3.5 Effect of humidity on local reduction of GO

Our experiments were carried out under an ambient environment, and water may condense on the sample surface during tip-sample contact. Then, possible effect of environmental humidity on the local reduction should be checked. The local thermal reduction was performed at relative humidity of 30%, 50% and 70% while keeping other conditions, but the generated SO features showed little difference (Fig.5), i.e. the humidity of 30%–70% is all right for the local thermal reduction of SO sheets.

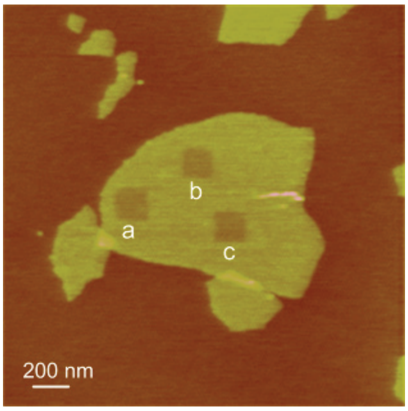

Fig.5 AFM image indicating the effect of relative humidity during local thermal reduction of GO. The three squares of 200 nm × 200 nm (a–c) were scanned with a same tip with temperature of 210°C for 4 times with a loading force of 145 nN. The relative humidity during heating was 30% (a), 50% (b), and 70% (c), respectively.

3.6 Characterization of the GO local reduction

The local thermal reduction of GO sheets was verified by LFM and SPFM[54–57]. Because the reduced GO shows lower friction coefficient, the LFM conveniently distinguishes the reduced area on the GO sheets[28,52]. In Fig.6(B), the two low-friction squares reduced previously can be seen clearly in the LFM image. Also, electric properties of GO sheet change after its local reduction. The SPFM image (Fig.6D) shows that the reduced areas of GO sheet and the mica substrate are in high contrast, differing significantly from the other regions.

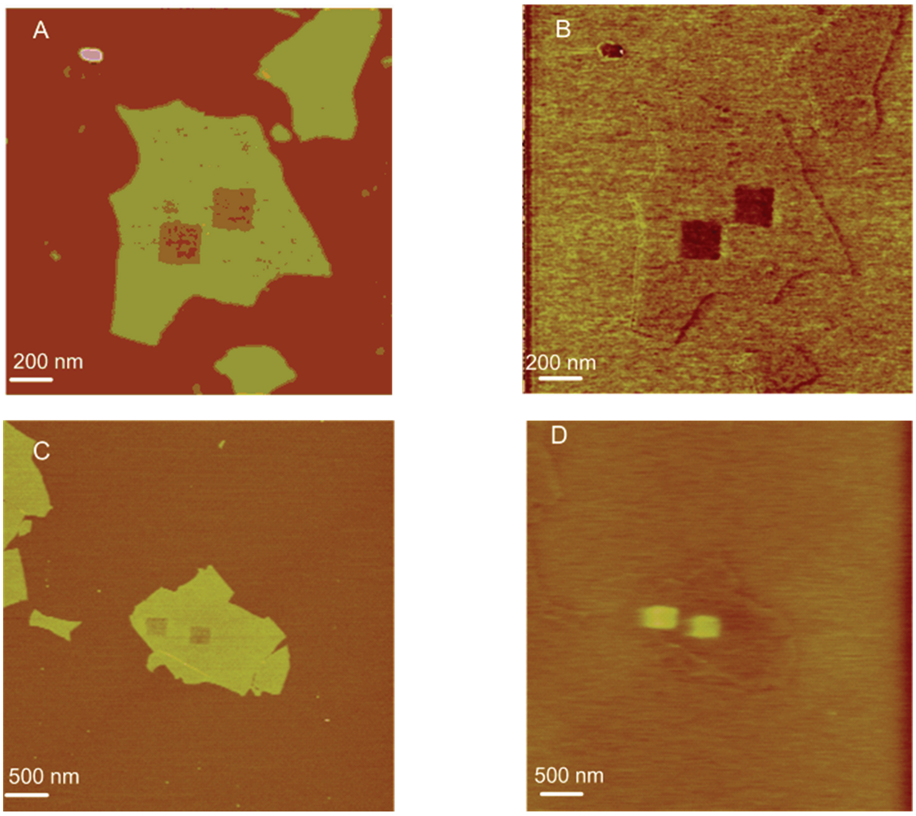

Fig.6 Height (A) and LFM (B) images indicating that the locally reduced regions of the GO sheet have lower friction coefficients. Height (C) and SPFM (D) images indicating that the locally reduced regions of the GO sheet are conductive.

4 Conclusions

In summary, we studied the factors affecting the local thermal reduction of GO, and found that the local thermal reduction was highly dependent on the tip temperature and heating time. Also, the loading force applied by the AFM tip during local heating plays important effects on the thermal reduction though it itself is not sufficient for local reduction of GO. The environmental humidity was found to slightly affect the local reduction in the relative humidity of 30% to 70%. These results are helpful for understanding the chemical origin of the local reduction of GO sheets, and for more controllable fabrication of reduced GO nanostructures for future applications.

Acknowledgments

This work was supported by National Basic Research Program of China (No. 2007CB936000), Chinese Academy of Sciences (No. KJCX2-EW-N03), and National Science Foundation of China (No. 10975175, 90923002, and 90923041). Y. Zhang thanks the Max Planck Society for support of a partner group.

References

1 Wallace P R. Phys Rev, 1947, **71:** 622–634.
2 McClure J W. Phys Rev, 1956, **104:** 666–671.
3 Semenoff G W. Phys Rev Lett, 1984, **53:** 2449–2452.
4 DiVincenzo D P, Mele E J. Phys Rev B, 1984, **29:** 1685–1694.
5 Novoselov K S, Geim A K, Morozov S V, *et al.* Sci, 2004, **306:** 666–669.

6 Novoselov K S, Geim A K, Morozov S, V *et al.* Nat, 2005, **438:** 197–200.

7 Zhang Y B, Tan Y W, Stormer H L, *et al.* Nat, 2005, **438:** 201–204.

8 Kopelevich Y, Esquinazi P. Adv Mater, 2007, **19:** 4559–4563.

9 Li X, Wang X, Zhang L, *et al.* Sci, 2008, **319:** 1229–1232.

10 Robinson J T, Zalalutdinov M, Baldwin J W, *et al.* Nano Lett, 2008, **8:** 3441–3445.

11 Stankovich S, Dikin D A, Dommett G H, *et al.* Nat, 2006, **442:** 282–286.

12 Geim A K, Novoselov K S. Nat Mater, 2007, **6:** 183–191.

13 Dong X C, Shi Y M, Huang W, *et al.* Adv Mater, 2010, **22:** 1649–1653.

14 Schedin F, Geim A K, Morozov S V, *et al.* Nat Mater, 2007, **6:** 652–655.

15 Mohanty N, Berry V. Nano Lett, 2008, **8:** 4469–4476.

16 Ang P K, Chen W, Wee A T S, *et al.* J Am Chem Soc, 2008, **130:** 14392–14393.

17 Wang Z J, Zhou X Z, Zhang J, *et al.* J Phys Chem C, 2009, **113:** 14071–14075.

18 He Q Y, Sudibya H G, Yin Z Y, *et al.* Acs Nano, 2010, **4:** 3201–3208.

19 Dikin D A, Stankovich S, Zimney E J, *et al.* Nat, 2007, **448:** 457–460.

20 Eda G, Fanchini G, Chhowalla M. Nat Nanotechnol, 2008, **3:** 270–274.

21 Tung V C, Allen M J, Yang Y, *et al.* Nat Nanotechnol, 2009, **4:** 25–29.

22 Li B, Cao XH, Ong H G, *et al.* Adv Mater, 2010, **22:** 3058–3061.

23 Tang Y B, Lee C S, Xu J, *et al.* Acs Nano, 2010, **4:** 3482–3488.

24 Valentini L, Cardinali M, Bon S B, *et al.* J Mater Chem, 2010, **20:** 10943–10943.

25 Valentini L, Cardinali M, Bon S B, *et al.* J Mater Chem, 2010, **20:** 995–1000.

26 Park S, Ruoff R S. Nat Nanotechnol, 2009, **4(4):** 217–224.

27 Li D, Muller M B, Gilje S, *et al.* Nat Nanotechnol, 2008, **3:** 101–105.

28 Wei Z, Wang D, Kim S, *et al.* Science, 2010, **328:** 1373–1376.

29 Zhang J, Yang H, Shen G, *et al.* Chem Commun (Camb), 2010, **46:** 1112–1114.

30 Si Y, Samulski E T. Nano Lett, 2008, **8:** 1679–1682.

31 Stankovich S, Dikin D A, Piner R D, *et al.* Carbon, 2007, **45:** 1558–1565.

32 Gilje S, Han S, Wang M, *et al.* Nano Lett, 2007, **7:** 3394–3398.

33 Becerril H A, Mao J, Liu Z, *et al.* Acs Nano, 2008, **2:** 463–470.

34 Gomez-Navarro C, Weitz R T, Bittner A M, *et al.* Nano Lett, 2007, **7:** 3499–3503.

35 Zhou X Z, Lu G, Qi X Y, *et al.* J Phys Chem C, 2009, **113:** 19119–19122.

36 Li H, Zhang J, Zhou X Z, *et al.* Langmuir, 2010, **26:** 5603–5609.

37 Li B, Lu G, Zhou X Z, *et al.* Langmuir, 2009, **25:** 10455–10458.

38 Duan H G, Xie E Q, Han L, *et al.* Adv Mater, 2008, **20:** 3284–3288.

39 Wei Z, Wang D, Kim S, *et al.* Sci, 2010, **328:** 1373–1376.

40 Wang D, Kim S, Underwood W D, *et al.* Appl Phys Lett, 2009, **95:** 2331081–2331083.

41 Wang D, Kodali V K, Underwood Ii W D, *et al.* Adv Funct Mater, 2009, **19:** 3696–3702.

42 Szoszkiewicz R, Okada T, Jones S C, *et al.* Nano Lett, 2007, **7:** 1064–1069.

43 Wang D B, Szoszkiewicz R, Lucas M, *et al.* Appl Phys Lett, 2007, **91:** 2431041–2431043.

44 Sheehan PE, Whitman L J, King W P, *et al.* Appl Phys Lett, 2004, **85:** 1589–1591.

45 Yang M, Sheehan P E, King W P, *et al.* J Am Chem Soc, 2006, **128:** 6774–6775.

46 Nelson B A, King W P, Laracuente A R, *et al.* Appl Phys Lett, 2006, **88:** 0331041–0331043.

47 Vettiger P, Cross G, Despont M, *et al.* Nanotechnol, IEEE Trans on, 2002, **1:** 39–55.

48 He H Y, Klinowski J, Forster M, *et al.* Chem Phys Lett, 1998, **287:** 53–56.

49 Schniepp H C, Li J L, McAllister M J, *et al.* J Phys Chem B, 2006, **110:** 8535–8539.

50 Hummers W S, Offeman R E. J Am Chem Soc, 1958, **80:** 1339–1339.

51 Nelson B A, King W P. Sensor Actuat A-Phys, 2007, **140:** 51–59.

52 Filleter T, McChesney J, Bostwick A, *et al.* Phys Rev Lett, 2009, **102:** 0861021–0861024.

53 Salmeron M. Oil Gas Sci Technol, 2001, **56:** 63–75.

54 Hu J, Xiao X D, Salmeron M. Appl Phys Lett, 1995, **67:** 476–478.

55 Hu J, Xiao X D, Ogletree D F, *et al.* Sci, 1995, **268:** 267–269.

56 Zhou X F, Sun J L, An H J, *et al.* Phys Rev E, 2005, **71:** 0629011–0629014.

57 Li X J, Sun J L, Zhou X F *et al.* J Vac Sci Technol B: Microelectron Nanometer Struct, 2003, **21:** 1070–1073.